Neuropilin-1 is required for vascular development and is a mediator of VEGF-dependent angiogenesis in zebrafish

Percy Lee*†, Katsutoshi Goishi*†, Alan J. Davidson‡, Robert Mannix*, Leonard Zon‡, and Michael Klagsbrun*§¶

Departments of *Surgical Research and §Pathology, and ‡Howard Hughes Medical Institute and Division of Hematology/Oncology, Children's Hospital and Harvard Medical School, Boston, MA 02115

Communicated by Patricia K. Donahoe, Massachusetts General Hospital, Boston, MA, June 19, 2002 (received for review March 15, 2002)

Neuropilin-1 (NRP1) is a cell-surface receptor for both vascular endothelial growth factor$_{165}$ (VEGF$_{165}$) and class 3 semaphorins that is expressed by neurons and endothelial cells. NRP1 is required for normal developmental angiogenesis in mice. The zebrafish is an excellent system for analyzing vascular development. Zebrafish intersegmental vessels correspond to mammalian capillary sprouts, whereas the axial vessels correspond to larger blood vessels, such as arteries. The zebrafish NRP1 gene (*znrp1*) was isolated and when overexpressed in cells, zNRP1 protein was a functional receptor for human VEGF$_{165}$. Whole-mount *in situ* hybridization showed that transcripts for *znrp1* during embryonic and early larval development were detected mainly in neuronal and vascular tissues. Morpholino-mediated knockdown of zNRP1 in embryos resulted in vascular defects, most notably impaired circulation in the intersegmental vessels. Circulation via trunk axial vessels was not affected. Embryos treated with VEGF receptor-2 kinase inhibitor had a similar intersegmental vessel defect suggesting that knockdown of zNRP1 reduces VEGF activity. To determine whether NRP1 and VEGF activities were interdependent *in vivo*, zNRP1 and VEGF morpholinos were coinjected into embryos at concentrations that individually did not significantly inhibit blood vessel development. The result was a potent inhibition of blood cell circulation via both intersegmental and axial vessels demonstrating that VEGF and NRP1 act synergistically to promote a functional circulatory system. These results provide the first physiological demonstration that NRP1 regulates angiogenesis through a VEGF-dependent pathway.

receptor kinase inhibitor | vasculogenesis | semaphorins | antisense morpholino

Neuropilin (NRP) is a 130- to 140-kDa membrane glycoprotein first identified in the optic tectum of *Xenopus laevis* and subsequently in the developing brain (1). Currently, there are two known *nrp* genes designated as *nrp1* and *nrp2* (2–4). NRP1 localizes to axons and was first identified as the receptor for Sema3A, a secreted axon guidance molecule that repels axons and collapses growth cones of dorsal root ganglia (3, 5). Recently, we identified NRP1 as a functional receptor for VEGF$_{165}$ (6), a potent angiogenesis factor essential for normal developmental angiogenesis (7, 8) and tumor angiogenesis (9). NRPs are the second class of VEGF receptors (VEGFRs) described so far, after the three receptor tyrosine kinases, VEGFR-1, VEGFR-2, and VEGFR-3 (10, 11). NRPs do not appear to be receptor kinases but may act as coreceptors for VEGFR-2 that enhance VEGF$_{165}$ activity (6).

There is ample evidence to suggest that NRP1 is involved in normal mouse vascular development as well as pathological angiogenesis, although the mechanism is unclear. It is expressed abundantly in endothelial cells (EC) of developing embryonic blood vessels (12). NRP1 knockout mice display abnormal axonal networks, deficiencies in neuronal vascularization, aortic arch malformations, and diminished and disorganized yolk sac vascularization (13, 14). Conversely, overexpression of NRP1 during mouse development results in excessive and abnormal blood vessel formation throughout the embryo (12). NRP1 is highly expressed by certain tumor cell types as the only VEGFR and contributes to tumor angiogenesis (6, 15). Conditional expression of NRP1 in tumor cells resulted in larger and more vascular tumors, possibly because of the increased concentration of NRP1-bound VEGF in the tumor.

To gain new insights into the function of NRPs in blood vessel development, we decided to study the vascular function of NRP in zebrafish. The zebrafish vascular system is advantageous for study because of the transparency of the embryos and the rapid development of a functional circulatory system (16). Functional analysis is facilitated by the ability to readily introduce small compounds into embryos to antagonize protein function—e.g., antisense morpholino oligonucleotides that specifically blocks a protein's translation (17) and VEGFR-2 kinase inhibitors that inhibit VEGF activity (18). Embryos treated with antisense morpholinos targeting VEGF showed a marked loss of developing blood vessels during vascular development (19).

Although NRP1 binds VEGF$_{165}$ *in vitro* and NRP1 is clearly required for mouse developmental angiogenesis, a question not yet resolved is whether VEGF activity depends on interactions with NRPs *in vivo*. We report here the cloning of the *znrp1* gene, its expression in development, and its functional characterization. Embryos microinjected with zNRP1 antisense morpholino oligonucleotides exhibited vascular defects including impaired circulation in the intersegmental vessels whereas circulation via trunk axial vessels was not affected. Coinjection of zNRP1 and zebrafish VEGF morpholinos at concentrations that individually did not inhibit blood vessel development significantly yielded a severe aberrant vascular phenotype including loss of both trunk axial and intersegmental vessel circulation. These results demonstrate that zebrafish VEGF activity is zNRP1 dependent. The results also provide a mechanism for the angiogenic properties of NRP1.

Materials and Methods

Zebrafish Maintenance. Zebrafish (Danio rerio) were maintained in the Children's Hospital breeding colony at 28.5°C on a 14 hr light/10 hr dark cycle. Embryos were collected from the natural mating of breeding pairs (AB), raised at 28.5°C, and staged as described (20). When necessary, embryos were anesthetized with 0.003% tricaine (Sigma). Embryos older than 24 h postfertilization (hpf) were raised in 0.2 mM 1-phenyl-2-thio-urea (Sigma) to prevent pigment formation.

Abbreviations: VEGF, vascular endothelial growth factor; VEGFR, VEGF receptor; DLAV, dorsal anastamosing longitudinal vessel; hpf, hours postfertilization; EC, endothelial cells; RACE, rapid amplification of cDNA ends.

Data deposition: The sequence reported in this paper has been deposited in the GenBank and EMBL databases (accession no. AY064213).

†P.L. and K.G. contributed equally to this work.

¶To whom reprint requests should be addressed. E-mail: michael.klagsbrun@tch.harvard.edu.

www.pnas.org/cgi/doi/10.1073/pnas.162366299

Cloning of Full-Length Zebrafish NRP1 cDNA. *Degenerate PCR.* Degenerate primers for NRP1 were made based on highly conserved amino acid sequences from rat, chicken, mouse, and human NRP1 (GIBCO). The forward primer was generated based on a consensus amino acid sequence DRLEIWD found in the NRP1 a domain (amino acids 208–214 of human NRP1). The reverse primer was generated based on a consensus amino acid sequence DECDDDQ found in the NRP1 c domain (amino acids 601–607 of human NRP1). An inosine residue was used at nucleotide positions where complete degeneracy was required. The forward primer sequence was 5′-GA(C/T)(A/C)GI(C/T)TIGA(A/G)ATIT-GGGA-3′. The reverse primer sequence was 5′-TG(A/G)TC (A/G)TC(A/G)TC(A/G)CA(C/T)TC(A/G)TC-3′. A PCR product ≈1.2 kb in size was cloned into the pGEM-T-easy vector (Promega) and sequenced.

5′- and 3′-rapid amplification of cDNA ends (RACE). Further 5′- and 3′-zebrafish NRP1 cDNA sequences were obtained by reverse transcription–PCR from 24 hpf embryo total RNA by using the SMART-RACE cDNA amplification kit (CLONTECH) according to the manufacturer's protocol. Specific primers used for 5′-RACE were: antisense 5′-RACE-A1, 5′-TTT-ATTCGTGTCCTCCAAAGGCGTCC-3′; and antisense nested 5′-RACE-A2, 5′-AGTTTCCATACCCAAAGGCTCAGTGC-3′. Similarly, specific primers used for 3′-RACE were: sense 3′-RACE-S1, 5′-TCATCCAGGGAGGCAAACACCGAGAT-3′; and sense nested 3′-RACE-S2, CAGCGTTGAGGACAAT-GGAGCCAGTG-3′.

Zebra fish NRP1 cDNA. A cDNA containing the putative zNRP1 ORF was generated by reverse transcription–PCR by using forward and reverse primers that bind zNRP1 cDNA in the 5′-untranslated region and 3′-untranslated region regions, respectively. The forward primer sequence was: zNRP1-LDS1: 5′-ATTACTCGTCTATTTCGCGGAACTGC-3′. The reverse primer sequence was: zNRP1-LDAS1: 5′-ACAGAGCCTT-GTCCTCCTCCAATC-3′. Reverse transcription–PCR by using cDNA generated from 24 hpf embryo total RNA as a template produced a single predicted 3.2-kb band that was directly cloned into the pGEM-T-easy vector (Promega) and the expression vector pCR3.1 (Invitrogen) to generate pGEM-T-easy-zNRP1 and pCR3.1-zNRP1, respectively. Both constructs were fully sequenced and compared to ensure sequence fidelity.

Western Blot and VEGF Binding. *Transfections.* Porcine aortic endothelial cells (6) were transfected with 1 μg of control vector (pCR 3.1) or pCR3.1-zNRP1 at ≈50% confluence by using the FuGene 6 transfection reagent (Roche Molecular Biochemicals) following the manufacturer's instructions.

Western blot. Cells (one 6-cm dish) and embryos (15 dechorionated 24 hpf embryos/sample) were lysed, incubated with Con A Sepharose beads, and analyzed by Western blot as described (21). NRP1 (130 kDa) was detected with rabbit anti-NRP1 antibody directed against the b2/c domain of mouse NRP1 obtained from H. Fujisawa (Nagoya, Japan), at 1:2000 dilution, overnight followed by incubation with horseradish peroxidase-conjugated secondary anti-rabbit IgG (1:10,000; Santa Cruz Biotechnology). Blots were developed by using an enhanced chemiluminescence kit (NEN).

VEGF crosslinking. $VEGF_{165}$ was radioiodinated (90,000 cpm/ng) and chemically cross-linked to porcine aortic endothelial cells with 200 μM disuccinimidyl suberate as described (6, 22). Cross-linked lysates were analyzed by 7.5% SDS/PAGE, and complexes containing ^{125}I-$VEGF_{165}$ were visualized by autoradiography.

Whole-Mount *in Situ* Hybridization. Expression of *znrp1* was detected by whole mount *in situ* hybridization as described (23). After the occurrence of a color reaction with alkaline phosphatase substrates, the embryos were mounted in glycerol and photographed. For embryos that were flat-mounted, the yolk was removed and the embryo flattened under a bridged coverslip for photography.

***In Vitro* Transcription and Translation.** *In vitro* transcription and translation of zNRP1 was performed by using the TNT Quick Coupled Reticulocyte Lysate system (Promega), according to the manufacturer's protocol with the following modifications: in a 25-μl reaction, 0.5 μg of pCR3.1-zNRP1 and various amounts of morpholino antisense oligos (0, 1 nM–10 μM final concentration) were added to the TNT Quick Master Mix that contained all of the required components for *in vitro* transcription and translation and incubated at 30°C for 90 min. Five microliters from the reaction mix were resolved by 7.5% SDS/PAGE, and S^{35}-labeled proteins were visualized by autoradiography.

Morpholinos. Morpholinos were designed with sequences complementary to *znrp1* cDNA in a location just upstream to the initiating start codon based on the company's recommendations. The morpholino sequences were: zNRP1 morpholino, 5′-GAATCCTGGAGTTCGGAGTGCGGAA-3′; zNRP1 4-base mismatch morpholino, 5′-GATTCCAGGAGTTCGGACTGC-CGAA-3′; and zebrafish VEGF morpholino, 5′-GTATCAAATA-AACAACCAAGTTCAT-3′. Morpholino antisense oligos were diluted in 5 mM Hepes pH 7.4. Morpholino solutions (150 pl) were injected into the blastomere of each embryo at the 1–4 cell stage. Four-base mismatch morpholinos and inert standard morpholinos, which have no effect on zebrafish development, were used as controls. Inert standard morpholino (0.125 mM, 5′-CCTCTTAC-CTCAGTTACAATTTATA-3′) tagged with fluorescein at the 3′-end was mixed into each sample to monitor success of injection and even distribution of morpholino in the embryos.

Kinase Inhibitors. The VEGFR-2 tyrosine kinase inhibitor PTK787/ZK 222584 (24) was kindly obtained from Novartis Pharma AG. Dechorionated zebrafish embryos were soaked in 3 ml of fish medium containing various concentrations of kinase inhibitor in 6-well plates.

Imaging. Zebrafish embryos were visualized with an Olympus SZX12 stereomicroscope and photographed by using an Olympus DP11 digital camera. To visualize blood vessels, microangiography was performed as described (19) with the following modifications: FITC-Dextran (Sigma) was solubilized in 75 mM NaCl solution and injected into the sinus venosa. For fluorescent microscopy, a FITC filter was used. For visualization of blood flow, zebrafish were magnified (×40) by using transmitted light on a Nikon Diaphot 300 inverted microscope and serial time-lapse images were collected by using a Hamamatsu (Middlesex, NJ) CCD digital camera (model 4742–95). The mean image intensity for these images was calculated on a pixel-by-pixel basis by using the IPLAB RATIOPLUS program (Scanalytics). Images depicting the variance from the mean were produced to display areas of movement, which corresponded to blood flow. These images were then pseudocolored within an intensity window to show areas of blood flow.

Results

Isolation of a Zebrafish nrp1 cDNA. To analyze the function of NRP during development, the zebrafish ortholog of *nrp (znrp)* was isolated by using degenerate primers, which were designed based on highly conserved human, mouse, rat, and chicken NRP1 amino acid sequences. The predicted zNRP ORF encodes a 923-aa protein, the same size as human NRP1. zNRP contains a 19-aa putative signal peptide, a relatively large 859-aa extracellular domain, a transmembrane domain, and a relatively short 40-aa cytoplasmic domain (not shown). Overall, zNRP is ≈64% identical to human and rat NRP1 and ≈45% identical to human NRP2. Based on these amino acid identities and the greater homology to mammalian *nrp1*, we have designated the *znrp* gene as *znrp1*.

Fig. 1. *In situ* hybridization of *znrp1* in the developing zebrafish. Expression of *znrp1* in zebrafish embryos at five somites (*A*), 22 somites (*B*), and 48 hpf (*C* and *D*). (*A*) Dorsal view of a flat-mounted embryo with anterior to the left. (*B–D*) Lateral views with anterior to the left. (*C Inset*) Dorsal view of the head with anterior to the left. (*A*) At the five-somite stage, *znrp1* is expressed in the hatching gland (asterisk), developing neural tube (arrowhead), and lateral plate mesoderm (arrows). (*B*) High magnification of the tail region of a 22-somite stage embryo. Cells expressing *znrp1* include tail angioblasts (black arrowhead), gut endoderm (white arrowhead), motoneurons (small black arrow), hypochord (large black arrow), and the ventromedial region of the somites (white arrow). In addition, *znrp1* transcripts are expressed by the yolk syncytial layer (YSL) in the yolk extension (asterisk). (*C*) At 48 hpf, *znrp1* is expressed extensively throughout the brain, the gut endoderm (white arrowhead), the pectoral fin buds (black arrowhead, *Inset*), and the vasculature in the trunk and tail. (*D*) High magnification of the tail region of a 48-h embryo showing *znrp1* expression in the major trunk vessels, caudal vein plexus (arrowhead), and intersegmental vessels (arrow).

Whole-Mount *in Situ* Hybridization of zNRP. The expression pattern of *znrp1* during embryonic and early larval development was examined by whole mount *in situ* hybridization (Fig. 1). Maternal transcripts for *znrp1* were ubiquitously distributed in the embryo until the early gastrula stage but by the end of gastrulation became localized to the yolk syncytial layer (not shown). During somitogenesis stages, *znrp1* showed a dynamic expression pattern with transcripts being detected in the hatching gland, notochord, central nervous system, cranial neural crest cells, somites, and lateral plate mesoderm (Fig. 1*A* and data not shown). By 22 somites (Fig. 1*B*), new sites of *znrp1* expression included angioblasts in the tail, gut endoderm, motoneurons, and hypochord. At this stage, transcripts of *znrp1* were restricted to the ventromedial regions of the somites. Between 24 and 36 hpf, the expression of *znrp1* within the vascular system expanded to include the endothelium of the major vessels in the trunk and tail (data not shown). At 48 hpf (Fig. 1 *C* and *D*), elaborate staining for *znrp1* was found in the brain, eyes, pectoral fin buds (Fig. 1*C Inset*), trunk, and tail vasculature (Fig. 1 *C* and *D*), as well as persisting in the gut endoderm (Fig. 1*C*). Within the trunk and tail vasculature, *znrp1* transcripts were detected in the endothelium of the dorsal aorta and posterior cardinal vein, the caudal vein plexus, and the intersegmental vessels in the tail (Fig. 1*D*).

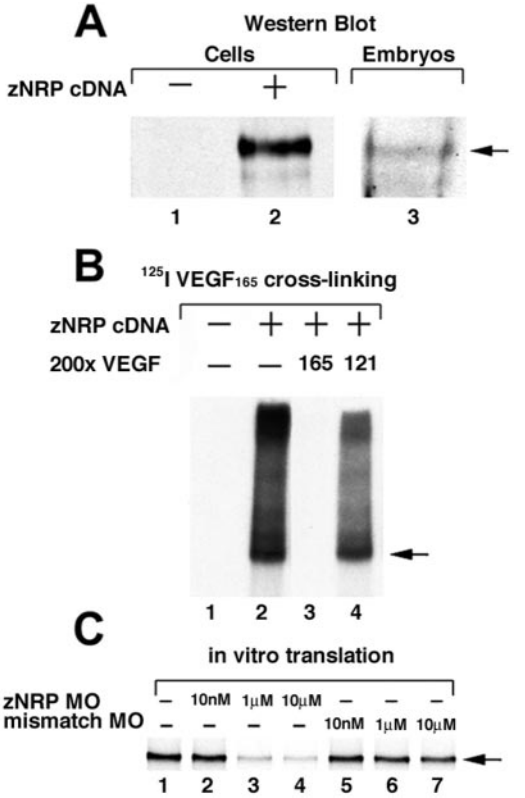

Fig. 2. zNRP1 is a functional VEGF receptor. (*A*) Western blot. Porcine aortic endothelial cells were transiently transfected with 1 μg of vector alone control (lane 1) or *znrp1* cDNA (lane 2) for $\approx$48 h. Cell lysates were analyzed by Western blot by using anti-NRP1 Ab. The arrow points to 140-kDa zNRP1. Lysates of 15 24-hpf wild-type zebrafish embryos were analyzed by Western blot (lane 3). (*B*) Cross-linking. Porcine aortic endothelial cells were transiently transfected with vector alone (lane 1) or 1 μg of zNRP1 cDNA (lane 2) and incubated with ^{125}I-VEGF$_{165}$ in the presence of disuccinimidyl suberate cross-linking reagent. Radioiodinated cross-linked complexes were resolved on SDS/PAGE and exposed to autoradiography film. Competition with unlabeled VEGF$_{165}$ (lane 3) and with unlabeled VEGF$_{121}$ (lane 4) are shown. Arrow points to 170-kDa complexes containing ^{125}I-VEGF$_{165}$ and zNRP1. (*C*) *In vitro* translation. zNRP1 cDNA (0.5 μg) was transcribed and translated *in vitro* in the presence of ^{35}S-labeled methionine in the absence of morpholino (lane 1) or in the presence of various concentrations of anti-zNRP1 morpholino (lanes 2–4) or 4-base mismatch control morpholino (lanes 5–7). ^{35}S-zNRP1 (arrow, 130 kDa) was analyzed by 7.5% SDS/PAGE followed by autoradiography.

zNRP1 Is a Functional Isoform-Specific Receptor for VEGF$_{165}$ and Not VEGF$_{121}$. To detect zNRP1 protein, Western blot was carried out by using an Ab directed against the extracellular domains of mouse NRP1. A 130- to 140-kDa zNRP1 protein was detected in EC transfected with *znrp1* cDNA (Fig. 2*A*, lane 2) and in lysates prepared from 24-hpf wild-type zebrafish embryos (Fig. 2*A*, lane 3). Furthermore, zNRP1 was shown to be a functional receptor. Human ^{125}I-VEGF$_{165}$ cross-linked EC transfected with *znrp1* cDNA (Fig. 2*B*, lane 2), but not vector alone (Fig. 2*B*, lane 1),

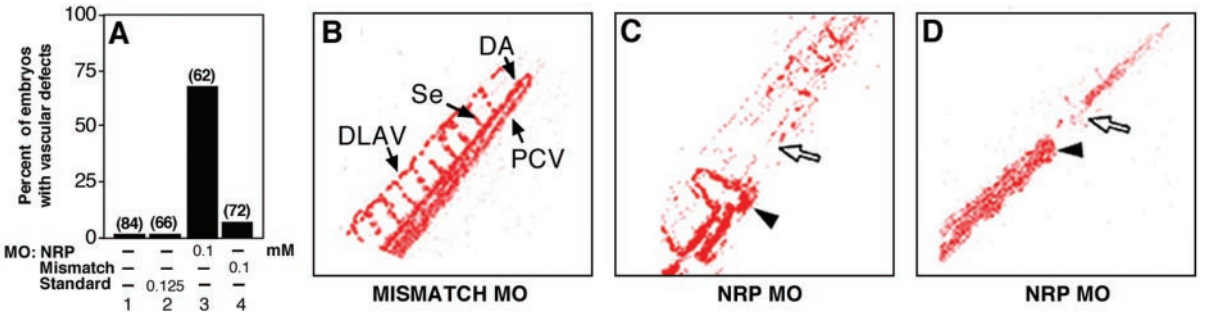

Fig. 3. zNRP1 morpholinos induce vascular defects. Anti-zNRP1 morpholinos and controls were injected directly into the blastomere of 1–4 cell stage embryos. (*A*) Percentage of morpholino-treated embryos and controls with vascular defects. The number of embryos injected is shown above the bars. (*B–D*) Areas of blood flow (colorized red) in 60-hpf embryos by using serial imaging methodology as described in *Materials and Methods*. (*B*) The 0.1 mM 4-base-mismatch control. Arrows depict dorsal aorta (DA), posterior cardinal vein (PCV), segmental vessels (Se), and DLAV. (*C* and *D*) Two representative embryos injected with 0.1 mM anti-zNRP1 morpholino. Arrowheads depict artery–vein connections (fistulas) in the vasculature. Open arrows depict areas in tail lacking blood flow.

to form a 165- to 175-kDa complex. The larger complexes at the top of the gel are most likely complexes of ^{125}I-VEGF$_{165}$ and multimers of zNRP1. Cross-linking with 200-fold molar of excess unlabeled VEGF$_{165}$ completely inhibited formation of the ^{125}I-VEGF$_{165}$/zNRP1 complex (Fig. 2*B*, lane 3) whereas cross-linking with 200-fold molar excess of unlabeled VEGF$_{121}$ did not (Fig. 2*B*, lane 4), consistent with the known isoform specificity of VEGF–NRP interactions (6).

Specific Morpholino Oligos Inhibit zNRP1 *in Vitro* Translation. Antisense morpholino oligos (morpholinos) are specific inhibitors of translation that act by binding to complementary sequences on mRNA and inhibiting access by ribosomes (17). Anti-zNRP1 morpholinos and control morpholinos with 4 of the 26 bases mutated (4-base mismatch) were synthesized. The potency and specificity of zNRP1 morpholinos were tested in an *in vitro* transcription and translation system. The zNRP1 morpholino oligos inhibited protein translation in a dose-dependent manner (Fig. 2*C*, lanes 2–4). Quantitation by densitometric analysis demonstrated that 1 and 10 μM morpholino inhibited zNRP1 translation by ≈75% and 87%, respectively. On the other hand, the inhibition by the control 4-base mismatch morpholinos was negligible, even at 10 μM (Fig. 2*C*, lanes 5–7).

Inhibition of zNRP1 Synthesis *in Vivo* Results in Vascular Defects. Zebrafish embryos were microinjected with 0.1 mM zNRP1 morpholinos at the 1–4 cell stage and examined for vascular defects at 24–48 hpf. The vascular defects included an accumulation of blood cells in the tail, short-circuited blood flow and lack of circulation in intersegmental vessels. Approximately 65–70% of the 62 zNRP1 morpholino-injected embryos tested (Fig. 3*A*, lane 3) had vascular defects as compared to 7% of the embryos injected with the 4-base mismatch control (Fig. 3*A*, lane 4) at the same concentrations. As further controls, uninjected embryos (Fig. 3*A*, lane 1) or embryos injected with an inert standard morpholino (Fig. 3*A*, lane 2) were not affected. Serial photomicrographs were used to produce images depicting the variance from the mean, thereby effectively depicting only the areas of active blood flow (Fig. 3 *B–D*). Embryos injected with 4-base mismatch control morpholinos (Fig. 3*B*) had normal blood cell circulation via axial (e.g., dorsal aorta, posterior cardinal vein) vessels, intersegmental vessels, and the dorsal anastamosing longitudinal vessels (DLAV). On the other hand, in embryos treated with zNRP1 morpholinos, the vascular bed appeared short-circuited and circulation was blocked in the tail beginning at ≈36 hpf (Fig. 3 *C* and *D*). In some cases, abnormal connections (fistulas) were formed between the artery and vein, which prematurely returned blood circulation back to the heart (Fig. 3*C*). Blood cells accumulated posterior to the abnormal fistulas. There was essentially no circulation in intersegmental vessels and the DLAV.

Blood vessel circulation also was analyzed by microangiography (Fig. 4). Embryos were injected with morpholinos and FITC-dextran was injected into the circulation through the cardinal veins of these embryos at ≈56 hpf to visualize blood vessels directly. At a concentration of 0.1 mM morpholino, approximately one-half of the embryos had defects including diminished circulation in the intersegmental vessels, in the DLAV and in the caudal vein plexus (Fig. 4*B*). On the other hand, circulation in the trunk axial vessels appeared normal. Preferential inhibitory effects on small but not large blood vessels occurred at higher morpholino concentrations as well. In contrast, all of the embryos injected with 4-base mismatch control morpholinos had normal blood vessels (Fig. 4*A*).

zNRP1 Mediates VEGF-Dependent Angiogenesis. Zebrafish were treated with a VEGFR-2 kinase inhibitor at 24 hpf, and circulation through the blood vessels was visualized by injection of FITC-dextran into the cardinal vein at 56 hpf. As was the case with zNRP1 morpholino treatment, there was a preferential inhibitory effect on intersegmental vessel/DLAV circulation compared to trunk vessels (Fig. 4*C*). EGFR and PDGFR kinase inhibitors did not induce an abnormal vascular phenotype (data not shown). These results suggested that zNRP1 knockdown might affect VEGF activity. To examine this possibility, zebrafish were coinjected with anti-zNRP1 and anti-VEGF morpholinos. It has previously been shown that antisense VEGF morpholinos inhibited blood vessel formation in zebrafish embryos in a dose-dependent manner (19). In confirmation, 1 mM VEGF morpholino inhibited both axial vessels and intersegmental vessel development (Fig. 4*D*). A lower concentration of VEGF morpholino (0.3 mM) was chosen which did not have any significant effect on blood vessel circulation (Fig. 4*E*). Of the 22 embryos injected with VEGF morpholino at this concentration, none (0/22) had defects in trunk axial vessel circulation and only 2/22 had defects in intersegmental vessel/DLAV circulation. A concentration of anti-zNRP1 morpholino (0.1 mM) was chosen that had no inhibitory effects on trunk axial vessels (0/14) and with inhibitory effects on intersegmental vessel and DLAV circulation in one-half of the 14 embryos (Fig. 4*B*). However, when embryos were coinjected with both morpholinos, all of the embryos (19/19) exhibited a total loss of the circulation throughout the trunk, both axial and intersegmental vessels (Fig. 4*F*). As a control, there were no vascular defects in the 13 embryos coinjected with zebrafish VEGF morpholino and the zNRP 4-base mismatch morpholino (Fig. 4*G*), demonstrating the contribution of zNRP1 to the vascular defects. Together these

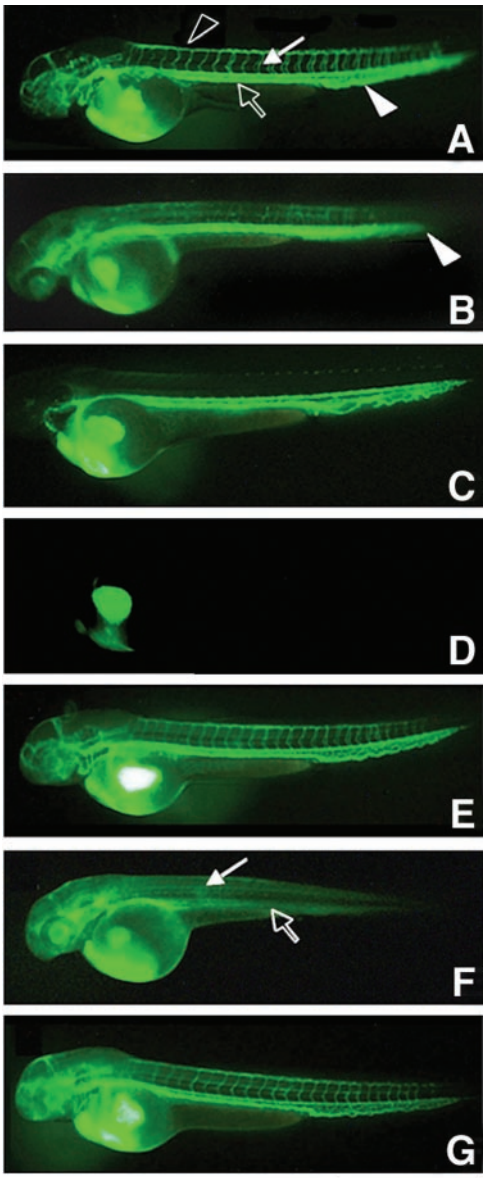

	Number of Embryos	Vascular defects Trunk	Se
A. NRP mismatch MO	5	0	0
B. NRP MO	14	0	7
C. PTK 787	30	0	30
D. VEGF MO (1 mM)	29	13	24
E. VEGF MO (0.3 mM)	22	0	2
F. NRP + VEGF MO	19	19	19
G. NRP mis MO + VEGF MO	13	0	0

Fig. 4. Microangiography of blood vessels. Embryos were injected with antisense morpholinos or controls at the 1–4 cell stage or soaked with VEGFR-2 kinase inhibitor at 24 h. Circulation through the blood vessels was visualized by injection of FITC-dextran into the cardinal vein at 56 hpf. Representative embryos are shown in each panel and a statistical analysis is shown at the bottom. (*A*) The 0.1 mM 4-base mismatch morpholino control. Circulation in vasculature is normal. Intersegmental vessels (white arrow), DLAV (black arrowhead), trunk axial arteries and veins (black arrow), and caudal vein plexus (white arrowhead). (*B*) The 0.1 mM anti-zNRP1 morpholino. Circulation via intersegmental vessels, DLAV, caudal vein plexus, and posterior tail (white arrowhead) is diminished. Axial vessel circulation is not affected. (*C*) VEGFR-2 kinase inhibitor (1 μM) was added at 24 hpf. Circulation via intersegmental vessels and DLAV is diminished. Axial vessel circulation is not affected. (*D*) The 1 mM anti-zebrafish VEGF morpholino. Circulation is severely diminished in both axial and intersegmental vessels. (*E*) The 0.3 mM anti-zebrafish VEGF morpholino. Axial and intersegmental vessel circulation is normal. (*F*) Coinjection of 0.1 mM anti-zNRP1 morpholino and 0.3 mM anti-zebrafish VEGF morpholino. Circulation through both axial and intersegmental vessels is severely diminished. White arrow and black arrows depict respectively, where intersegmental vessels/DLAV and axial vessels are normally found but absent here. (*G*) Coinjection with 0.1 mM 4-base mismatch zNRP1 control morpholino and 0.3 mM anti-zebrafish VEGF morpholino. Circulation via axial and intersegmental vessel circulation is normal. (*Bottom*) From 5 to 30 embryos were injected in each sample group and scored for vascular defects. Trunk refers to the axial vessels in the trunk and Se refers to intersegmental vessels.

results suggest that zebrafish VEGF and zNRP1 cooperate in maintaining trunk axial and intersegmental vessel function.

Discussion

NRP1 plays an important role in regulating developmental angiogenesis (12–14). It binds $VEGF_{165}$ but has no known kinase activity. To understand the mechanisms by which NRP1 regulates angiogenesis, about which little is known, we have analyzed NRP1 function in zebrafish. In this report, we describe the isolation, expression, and functional analysis of the zebrafish ortholog of the *nrp1* gene as an isoform-specific receptor for $VEGF_{165}$. Furthermore, we demonstrate that angiogenesis in the zebrafish is mediated by VEGF–zNRP1 interactions *in vivo*.

zNRP1 is expressed mainly in neuronal and vascular tissues during embryogenesis. During formation of the vascular system, transcripts for *znrp1* are first expressed by tail angioblasts toward the end of somitogenesis and then become more widespread to include the endothelium of the major trunk vessels and intersegmental vessels by 48 hpf. To determine zNRP1 function, we used antisense morpholino oligos to inhibit protein synthesis (17). The knockdown of zNRP1 resulted in several vascular defects. The smaller blood vessels, corresponding to capillaries in particular, were affected. For example, there was diminished circulation in the intersegmental vessels and in the DLAV. Circulation also was diminished in the caudal vein plexus of the posterior tail. On the other hand, circulation via the larger trunk vessels—e.g., the dorsal aorta was not inhibited. There were some cases where circulation was short-circuited in the tail as a result of abnormal artery–vein connections, consistent with lack of a functional caudal vein plexus that normally connects the dorsal aorta and axial vein.

What are the possible explanations for the vascular defects seen in the zNRP1-deficient embryos? Cardiac contractility and size appeared to be normal; no obstruction of the aortic outflow tract was observed; and circulation via the trunk axial vessels was normal as analyzed by FITC dextran microangiography and by observing red blood cells circulating at a normal rate. Furthermore, the axial vessels were not affected, even though the morpholinos were administered at the 1–2 cell stage, before development of the axial vessels. On the other hand, zNRP1 deficiency resulted in a defect in the intersegmental vessels in which circulation was diminished. The nature of the defect is not clear. *In situ* hybridization analysis indicated that VEGFR-2 was expressed in the intersegmental vessel EC, suggesting that the EC are viable and that intact EC tubes might be present. However, even if tubes were present, they must be immature and nonfunctional because there was no blood flow via the intersegmental vessels whereas there was normal blood flow in the axial vessels. The differential effects of zNRP1 deficiency on small vs. large vessels may occur because they are products of different processes. The larger axial arteries and veins arise from the process of vasculogenesis, which involves the differentiation of precursor cells into EC, a process that occurs early in zebrafish development within hours. On the other hand, the small blood vessels are generated later by the process of angiogenesis, which

represents sprouting and branching from preexisting axial blood vessels. Intersegmental vessels begin to sprout from the preexisting dorsal aorta at ≈24 h (25). Recently, we showed that a double knockout of mouse NRP1 and NRP2 was characterized by lack of blood vessel branching in the yolk sac and diminished small blood vessel sprouting and lack of capillary plexus formation in the embryo (26), consistent with the zNRP1 morpholino phenotype. Furthermore, it was possible to rescue defective vascular development and angiogenesis in NRP1-deficient mouse embryos and in *para*-aortic explants prepared from these mice with a dimer of soluble NRP1 (27). Together, it is plausible that zNRP1 plays a role in sprouting of a functionally mature smaller vessel network that enables circulation to occur through these vessels, but not in development of the larger axial vessels.

That zNRP1 knockdown affects VEGF activity is plausible because zNRP1 binds $VEGF_{165}$. A VEGFR-2 kinase inhibitor administered at 24 hpf when intersegmental vessel sprouting begins, and analyzed at 56 hpf, had a vascular phenotype similar to that of zNRP1 morpholino-treated embryos analyzed at 56 hpf—i.e., circulation was inhibited in intersegmental vessels and the DLAV but not in trunk axial vessels. A similar result by using the same kinase inhibitor, PTK787/ZK 222584, was recently reported (28). These results suggested that loss of zNRP1 synthesis had similar effects on zebrafish intersegmental vasculature as did loss of VEGF activity mediated by VEGFR-2.

To examine the possibility that NRP1 and VEGF function might be interdependent, we analyzed the effects of coinjecting NRP1 morpholinos and VEGF morpholinos at concentrations that individually did not significantly inhibit blood vessel development. The result was a complete impairment in both trunk axial vessel and intersegmental vessel circulation. Thus, it appears that the ability of VEGF to mediate zebrafish embryonic blood vessel development depends on cooperation with zNRP1. We propose that in the presence of normal VEGF levels, the formation of intersegmental vessels require zNRP1 whereas the larger axial vessels are formed even if zNRP1 is not available. However, when VEGF availability is reduced, the formation of the trunk axial vessels is zNRP1-dependent. Previously, we demonstrated *in vitro* that NRP1 was a coreceptor for VEGFR-2 in EC that enhanced $VEGF_{165}$ binding to VEGFR-2 (6). A possible mechanism in zebrafish is that the expression of zNRP1 lowers the concentration of VEGF required for activating VEGFR-2 to promote vasculogenesis and angiogenesis. The concentration dependence of VEGF *in vivo* is well established (7, 8). The possibility that zNRP1 deficiency might affect semaphorin activity has not been tested.

In summary, our studies provide an *in vivo* physiological demonstration that zebrafish VEGF activity is NRP1 dependent. The results also provide a mechanism by which NRP1 promotes developmental angiogenesis through its interaction with $VEGF_{165}$.

We thank Drs. Roni Mamluk, Diane Bielenberg, and Diane Bovenkamp for critical review of this manuscript, Drs. Nate Bahary and Barry Paw for very helpful discussions, Eric Santiestevan and Karim Awad for preparation of figures, and Alexandra Grady and Brenda Figueroa for preparation of the manuscript. We thank Dr. Cecilia Moens (Fred Hutchinson Cancer Research Center, Seattle) for helping with the interpretation of the *nrp* ISH expression patterns. This work was supported by National Institutes of Health Grants CA37392 and CA45448 (to M.K.) and H148801 and DK49216 (to L.Z.). P.L. is supported by a Howard Hughes Medical Institute Fellowship for medical students and by the Harvard Medical School, Massachusetts Institute of Technology, Division of Health Sciences and Technology research funding for medical students. K.G. is supported in part by the Departments of Obstetrics and Gynecology, Asahikawa Medical College, Asahikawa, Japan. L.Z. is supported by the Howard Hughes Medical Institute.

1. Kawakami, A., Kitsukawa, T., Takagi, S. & Fujisawa, H. (1996) *J. Neurobiol.* **29,** 1–17.
2. Chen, H., Chedotal, A., He, Z., Goodman, C. S. & Tessier-Lavigne, M. (1997) *Neuron* **19,** 547–559.
3. He, Z. & Tessier-Lavigne, M. (1997) *Cell* **90,** 739–751.
4. Rossignol, M., Gagnon, M. L. & Klagsbrun, M. (2000) *Genomics* **70,** 211–222.
5. Kolodkin, A. L., Levengood, D. V., Rowe, E. G., Tai, Y. T., Giger, R. J. & Ginty, D. D. (1997) *Cell* **90,** 753–762.
6. Soker, S., Takashima, S., Miao, H. Q., Neufeld, G. & Klagsbrun, M. (1998) *Cell* **92,** 735–745.
7. Carmeliet, P., Ferreira, V., Breier, G., Pollefeyt, S., Kieckens, L., Gertsenstein, M., Fahrig, M., Vandenhoeck, A., Harpal, K., Eberhardt, C., *et al.* (1996) *Nature (London)* **380,** 435–439.
8. Ferrara, N., Carver-Moore, K., Chen, H., Dowd, M., Lu, L., O'Shea, K. S., Powell-Braxton, L., Hillan, K. J. & Moore, M. W. (1996) *Nature (London)* **380,** 439–442.
9. Kim, K. J., Li, B., Winer, J., Armanini, M., Gillett, N., Phillips, H. S. & Ferrara, N. (1993) *Nature (London)* **362,** 841–844.
10. Ferrara, N. & Alitalo, K. (1999) *Nat. Med.* **5,** 1359–1364.
11. Neufeld, G., Cohen, T., Gengrinovitch, S. & Poltorak, Z. (1999) *FASEB J.* **13,** 9–22.
12. Kitsukawa, T., Shimono, A., Kawakami, A., Kondoh, H. & Fujisawa, H. (1995) *Development (Cambridge, U.K.)* **121,** 4309–4318.
13. Kawasaki, T., Kitsukawa, T., Bekku, Y., Matsuda, Y., Sanbo, M., Yagi, T. & Fujisawa, H. (1999) *Development (Cambridge, U.K.)* **126,** 4895–4902.
14. Kitsukawa, T., Shimizu, M., Sanbo, M., Hirata, T., Taniguchi, M., Bekku, Y., Yagi, T. & Fujisawa, H. (1997) *Neuron* **19,** 995–1005.
15. Miao, H. Q., Lee, P., Lin, H., Soker, S. & Klagsbrun, M. (2000) *FASEB J.* **14,** 2532–2539.
16. Isogai, S., Horiguchi, M. & Weinstein, B. M. (2001) *Dev. Biol.* **230,** 278–301.
17. Nasevicius, A. & Ekker, S. C. (2000) *Nat. Genet.* **26,** 216–220.
18. Serbedzija, G., Flynn, E. & Willett, C. (1999) *Angiogenesis* **3,** 353–359.
19. Nasevicius, A., Larson, J. & Ekker, S. C. (2000) *Yeast* **17,** 294–301.
20. Kimmel, C. B., Ballard, W. W., Kimmel, S. R., Ullmann, B. & Schilling, T. F. (1995) *Dev. Dyn.* **203,** 253–310.
21. Gagnon, M. L., Bielenberg, D. R., Gechtman, Z., Miao, H. Q., Takashima, S., Soker, S. & Klagsbrun, M. (2000) *Proc. Natl. Acad. Sci. USA* **97,** 2573–2578.
22. Soker, S., Fidder, H., Neufeld, G. & Klagsbrun, M. (1996) *J. Biol. Chem.* **271,** 5761–5767.
23. Thisse, C., Thisse, B., Halpern, M. E. & Postlethwait, J. H. (1994) *Dev. Biol.* **164,** 420–429.
24. Drevs, J., Hofmann, I., Hugenschmidt, H., Wittig, C., Madjar, H., Muller, M., Wood, J., Martiny-Baron, G., Unger, C. & Marme, D. (2000) *Cancer Res.* **60,** 4819–4824.
25. Childs, S., Chen, J. N., Garrity, D. M. & Fishman, M. C. (2002) *Development (Cambridge, U.K.)* **129,** 973–982.
26. Takashima, S., Kitakaze, M., Asakura, M., Asanuma, H., Sanada, S., Tashiro, F., Niwa, H., Miyazaki, J., Hirota, S., Kitamura, Y., *et al.* (2002) *Proc. Natl. Acad. Sci. USA* **99,** 3657–3662.
27. Yamada, Y., Takakura N., Yasue H., Fujisawa, H. & Suda, T. (2001) *Blood* **97,** 1671–1678.
28. Chan, J., Bayliss, P. E., Wood, J. M. & Roberts, T. M. (2002) *Cancer Cells* **1,** 257–267.